Heliyon

Received:
7 October 2016
Revised:
27 February 2017
Accepted:
25 May 2017

Cite as: Michael Brenner, Sakineh Esmaeili Mohsen Abadi, Ramin Balouchzadeh, H. Felix Lee, Hoo Sang Ko, Michael Johns, Nehal Malik, Joshua J. Lee, Guim Kwon. Estimation of insulin secretion, glucose uptake by tissues, and liver handling of glucose using a mathematical model of glucose-insulin homeostasis in lean and obese mice. Heliyon 3 (2017) e00310. doi: 10.1016/j.heliyon.2017.e00310

Estimation of insulin secretion, glucose uptake by tissues, and liver handling of glucose using a mathematical model of glucose-insulin homeostasis in lean and obese mice

Michael Brenner [a,1], **Sakineh Esmaeili Mohsen Abadi** [a,1], **Ramin Balouchzadeh** [a], **H. Felix Lee** [a], **Hoo Sang Ko** [a], **Michael Johns** [c], **Nehal Malik** [c], **Joshua J. Lee** [b], **Guim Kwon** [b,*]

[a] *Department of Mechanical and Industrial Engineering, Southern Illinois University Edwardsville, Edwardsville, IL 62026, United States*

[b] *School of Pharmacy, Southern Illinois University Edwardsville, Edwardsville, IL 62026, United States*

[c] *Department of Biological Sciences, Southern Illinois University Edwardsville, Edwardsville, IL 62026, United States*

* Corresponding author at: Department of Pharmaceutical Sciences, School of Pharmacy, Southern Illinois University Edwardsville, 220 University Park, Edwardsville, IL 62026–2000.

E-mail address: gkwon@siue.edu (G. Kwon).

[1] M. Brenner and S. E. M. Abadi contributed equally to this work.

Abstract

Destruction of the insulin-producing β-cells is the key determinant of diabetes mellitus regardless of their types. Due to their anatomical location within the islets of Langerhans scattered throughout the pancreas, it is difficult to monitor β-cell function and mass clinically. To this end, we propose to use a mathematical model of glucose-insulin homeostasis to estimate insulin secretion, glucose uptake by tissues, and hepatic handling of glucose. We applied the mathematical model by Lombarte et al. (2013) to compare various rate constants representing glucose-insulin homeostasis between lean (11% fat)- and high fat diet (HFD; 45% fat)-fed mice. Mice fed HFD (n = 12) for 3 months showed significantly higher body

http://dx.doi.org/10.1016/j.heliyon.2017.e00310

weights (49.97 ± 0.52 g vs. 29.86 ± 0.46 g), fasting blood glucose levels (213.08 ± 10.35 mg/dl vs. 121.91 ± 2.26 mg/dl), and glucose intolerance compared to mice fed lean diet (n = 12). Mice were injected with 1 g/kg glucose intraperitoneally and blood glucose levels were measured at various intervals for 120 min. We performed simulation using Arena^{TM} software based on the mathematical model and estimated the rate constants (9 parameters) for various terms in the differential equations using OptQuest^{TM}. The simulated data fit accurately to the observed data for both lean and obese mice, validating the use of the mathematical model in mice at different stages of diabetes progression. Among 9 parameters, 5 parameters including basal insulin, k_2 (rate constant for insulin-dependent glucose uptake to tissues), k_3 (rate constant for insulin-independent glucose uptake to tissues), k_4 (rate constant for liver glucose transfer), and I_{pi} (rate constant for insulin concentration where liver switches from glucose release to uptake) were significantly different between lean- and HFD-fed mice. Basal blood insulin levels, k_3, and I_{pi} were significantly elevated but k_2 and k_4 were reduced in mice fed a HFD compared to those fed a lean diet. Non-invasive assessment of the key components of glucose-insulin homeostasis including insulin secretion, glucose uptake by tissues, and hepatic handling of glucose may be helpful for individualized drug therapy and designing a customized control algorithm for the artificial pancreas.

Keywords: Mathematical bioscience

1. Introduction

Diabetes Mellitus is a widespread disease currently affecting 29.1 million Americans, or 9.3% of the total population (American Diabetes Association 2012 statistics). Furthermore, additional 86 million Americans are considered pre-diabetic, implying an alarming growth rate of the diabetes epidemic in the future. Two major forms of diabetes are type 1 and type 2 diabetes mellitus (T1DM and T2DM). T1DM is a chronic, progressive autoimmune disease caused by selective destruction of insulin-producing β-cells within the pancreatic islets of Langerhans [1]. Insulin delivered through an insulin pump or daily injections is essential to sustain life for these patients. The onset of T1DM occurs at an early age (young children and teens), hence, previously called juvenile diabetes. Even though T1DM comprises only 5–10% of diabetic patients, incidence of T1DM is rising at 3% per year [2] and the burden of the disease affecting children at young ages extending throughout their lives is enormous. Despite careful monitoring, a subset of patients with complicated T1DM are at high risk of life-threatening hypoglycemia episodes. Emerging new treatments for these patients include β-cell replacement therapy and closed-loop artificial pancreas device (APD) systems. The APD systems are externally worn medical devices under development, which consists of 3 components including continuous glucose monitoring sensor, insulin pump, and

http://dx.doi.org/10.1016/j.heliyon.2017.e00310

controller that determines insulin doses needed to maintain optimal blood glucose levels without input of patients. Recent advancements in technology enabled patients to use sophisticated insulin pumps that regulate insulin delivery at any desired rates and ever improving continuous glucose monitoring sensors that accurately measure blood glucose levels. Developing algorithms for the controller that determines insulin doses is an area that needs to be advanced along with the hardware of the APD systems. Individually customized adjustable algorithms may be necessary to provide a true artificial pancreas. Ability to estimate various parameters that regulate glucose and insulin homeostasis in an individual may contribute to developing such algorithms.

T2DM is the more prevalent form, comprising 90–95% of the diabetic patients. The causes of T2DM include a mixture of genetic predisposition, behavioral, and environmental risks. Among these, obesity is one of the primary risk factors that cause T2DM. The link between obesity and T2DM involves proinflammatory cytokines (tumor necrosis factor and interleukin-6), insulin resistance, glucolipotoxicity associated with nutrient overload, and alterations in cellular processes such as mitochondrial dysfuncton and endoplasmic reticulum stress [3, 4, 5, 6]. Treatments for T2DM include diet/exercise, oral hypoglycemic medications, and injectable agents including insulin and incretin mimetics. Oral hypoglycemic medications include secretagogues that stimulate insulin secretion from pancreatic β-cells, insulin sensitizers that enhance insulin action in the peripheral tissues, drugs that slow down glucose absorption from the gastro-intestinal tracts, and newer drugs that inhibit glucose reabsorption from the kidneys. Due to the progressive nature of the disease, patients with T2DM have different levels of reserved β-cell mass. At diagnosis of T2DM, β-cell mass is already reduced to ~50% (ranged 38%-63% depending on the studies [7, 8]), and further deterioration occurs over time. Evidence indicated that prolonged usage of secretagogues such as sulfonylurea causes β-cell fatigue, fastening the progression of the disease, which may place high risks especially in patients with low β-cell reserve [9, 10, 11]. Thus, individualized drug therapy based on reserved β-cell mass and severity of insulin resistance may delay the progression of the disease by preserving β-cell function and mass.

Clinical measurement of reserved β-cell mass and insulin resistance in a patient, however, is challenging. Due to the anatomical location of the islets of Langerhans scattered throughout the pancreas and its low tissue mass (~5% of the pancreas), conventional noninvasive imaging techniques such as computed tomography (CT) and magnetic resonance imaging (MRI) are inadequate due to low signal. Despite considerable research effort over the last decade, technologies for noninvasive imaging of β-cells have not yet reached to clinical application. The homeostasis model assessment (HOMA) is often used to evaluate pancreatic β-cell function (HOMA-β) and insulin resistance (HOMA-IR). HOMA-β and HOMA-IR are

http://dx.doi.org/10.1016/j.heliyon.2017.e00310

calculated based on fasting blood glucose and insulin levels [12] However, there are two major limitations of this approach: 1) fasting glucose and insulin levels in patients treated with hypoglycemic agents and/or insulin do not truly reflect the state of reserved β-cell mass, and 2) the reduction in postprandial rather than fasting insulin secretion is more prominent in the progression of T2DM. Alternatively, postprandial C-peptide to glucose ratio after oral glucose ingestion is proposed to be a better marker for pancreatic β-cell mass [13].

We investigated the feasibility of estimating insulin secretion, glucose uptake by tissues, and liver handling of glucose using a mathematical model of glucose-insulin homeostasis and the blood glucose levels after intra-peritoneal glucose injection. The mathematical model consisting of three differential equations and 9 parameters that describe key components of glucose-insulin homeostasis was first reported and validated in healthy rats by Lomarte et al. [14]. Accurate estimation of the rate constants determine glucose-insulin homeostasis in patients may be used for customized drug therapy for patients with T2DM as well as developing individually customized algorithms for the APD systems for patients with T1DM and subpopulations of T2DM.

2. Materials and methods

2.1. Animals

Male B6D2F1 mice (the F1 hybrids of C57BL/6 and DBA/2, 4–6 weeks) were purchased from Harlan Sprague-Dawley (Indianapolis, IN) and were maintained in our animal facility under controlled conditions (temperature 68–73 °F and 12 h light-dark cycle). Male B62DF1 mice have been shown to develop diabetic symptoms characterized by hyperglycemia, glucosuria, elevated hemoglobin A1C levels, and progressive structural and functional islet defects after 3 to 4 months of HFD feeding [15]. After a one week acclimation period, the mice (4 per cage) were fed for 3 months with a commercial lean chow diet (13.4% kcal fat, El-Mel, St. Louis, MO) or a HFD (45% kcal fat, Harlan laboratories, Madison, WI) and water *ad libitum*. After a 3 month diet period, body weights and fasting blood glucose levels were determined, followed by intraperitoneal glucose tolerance test (IPGTT). All animal maintenance and treatment protocols complied with the Guide for Care and Use of Laboratory Animals as adopted by the National Institute of Health and approved by the Southern Illinois University Edwardsville (SIUE) Institutional Animal Care and Use Committee (IACUC).

2.2. Intra-peritoneal glucose tolerance test

Mice were fasted for 5 h and administered 1 g/kg glucose by intra-peritoneal injection using sterile 27 G disposable needles. Blood glucose levels were determined using Contour glucose meter collecting blood from the tip of the tail at

http://dx.doi.org/10.1016/j.heliyon.2017.e00310

0 (prior to glucose injection) and every minute for the first 16 min, every 2 min for the next 14 min, every 5 min until 1 h, and then every 15 min until 2 h. The frequency of blood glucose measurement was determined based on our previous studies that showed the peak occurs between ~15–30 min after glucose injection, followed by steady declining to basal or above basal levels. Frequent glucose measurement every 1 or 2 min during the first 30 min allowed us to capture the deflection of the blood glucose peak accurately.

2.3. Plasma insulin levels

A 1:10 dilution of plasma was assayed for insulin content by radioimmunoassay (RIA) kit (Millipore) following the manufacturer's instructions. Basal insulin levels of lean and HFD-fed mice were determined to be ~300 pmol/l and ~1000 pmol/l, respectively, which were used as initial values for the simulations.

2.4. Mathematical model

We used the mathematical model of glucose-insulin homeostasis originally proposed by Lombarte et al. [14] to study the extent to which the parameters determine glucose-insulin homeostasis differ between lean and HFD-fed mice. The proposed model consists of three differential equations that describe the changes of blood glucose (G), blood insulin (I), and the amount of glucose (D) in the peritoneal cavity over time.

$$dG/dt = -k_4(I - I_{pi}) - k_2I - k_3 + k_0D \quad (1)$$

$$dI/dt = k_1G - k_6I \quad (2)$$

$$dD/dt = -k_aD \quad (3)$$

Equation (1) represents the change of blood glucose concentration over time. The term $k_4(I - I_{pi})$ represents the hepatic handling of glucose. The liver extracts ~1/3 of postprandial blood glucose, which is used for production of energy to maintain liver function and synthesis of glycogen and lipids as energy reserve. Between meals and during sleep when blood glucose levels decrease below an optimal range (70–130 mg/dl), the liver releases glucose into the blood stream via gluconeogenesis and glycogenololysis. The term $k_4(I - I_{pi})$, thus, is positive when glucose is taken up into the liver (when $I > I_{pi}$) but negative when glucose is released into the circulation from the liver (when $I < I_{pi}$). I represents blood insulin concentration, I_{pi} represents blood insulin concentration when the liver changes from the release to the uptake of glucose, and k_4 is the rate constant of uptake or release of glucose by the liver as described in the original paper by Lombarte et al. [14]. The k_2I term represents the insulin-dependent glucose uptake by the tissues including muscle, adipocytes, and liver. The k_3 term represents the insulin-independent glucose uptake by the tissues such as neuronal cells in the brain and white blood cells in the

http://dx.doi.org/10.1016/j.heliyon.2017.e00310

circulation [16, 17]. The k_0D term represents the change in blood glucose concentration due to the intra-peritoneal injection of glucose.

Equation (2) represents the change of blood insulin concentration over time. The term k_1G represents the pancreatic insulin secretion, which is regulated primarily by blood glucose concentration. The k_6I term represents blood insulin clearance. The liver is the primary site of insulin clearance. Approximately 80% of insulin is removed by the liver and the remainder is cleared by the kidneys and muscles [18].

Equation (3) represents the change of glucose in the peritoneal cavity. Of note, the definition of D in the present paper is the amount of glucose in the peritoneal cavity, not the intestine because we administered glucose via intra-peritoneal injection rather than per orally as describe in the original paper. Thus, the term k_a represents a rate constant of glucose leaving the peritoneal cavity, not the intestine.

2.5. Mathematical analysis and parameter estimation

Detailed descriptions of mathematical analysis and parameter estimation are reported in the original paper by Lombarte et al. [14]. Since we adopted the same model, mathematical analysis and parameter estimation are identical,

2.6. Simulation and optimization of the rate constants

We used Arena^{TM} simulation (a program by Rockwell Software) combined with the OptQuest^{TM} toolset to evaluate the mathematical model and optimally estimate the parameters. We developed a simulation program which incorporated the observed values in our experiments, glucose injections and initial parameter values as the simulation inputs. Using the inputs, the program created a continuous prediction of both insulin and glucose levels The search algorithm of OptQuest^{TM} evaluated various combinations of parameters and determined the best set that minimized the sum of squared errors between the observed and the simulated data.

2.7. Statistical analysis

Results are expressed as mean ± SEM. Differences between means were evaluated using the Wilcoxon-Mann-Whitney test because the distribution of the data for some parameters were not normally distributed. Significant differences are indicated by *$p < 0.05$, **$p < 0.01$, ***$p < 0.001$, ****$p < 0.0001$.

3. Results and discussions

Obesity is one of the primary risk factors for T2DM. We induced obesity in B6D2F1 mice by feeding a HFD for 3 months and compared the key parameters that determine glucose-insulin homeostasis between lean- and HFD-fed mice. Fig. 1A shows that the bodyweights of the mice fed the HFD (49.97 ± 0.52 g) were

http://dx.doi.org/10.1016/j.heliyon.2017.e00310

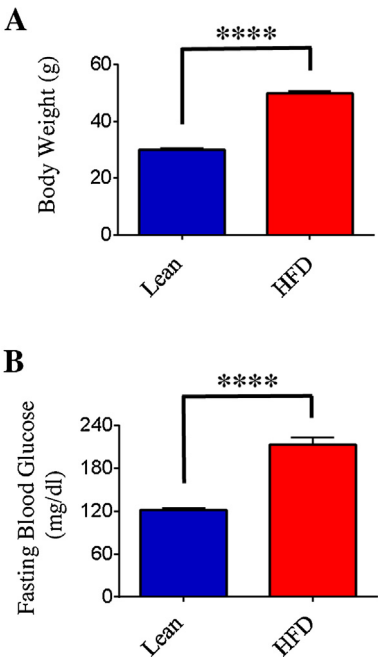

Fig. 1. (A) Mean body weights and (B) fasting blood glucose levels of B6D2F1 mice 3 months after lean- or high fat-diet. Mice were fasted for 5 h prior to determination of fasting blood glucose levels. Values are presented as means ± SEM. (n = 12).

significantly higher than those fed the lean diet (29.86 ± 0.46 g). Increases in the body weights, as anticipated, were accompanied by significantly higher fasting blood glucose levels in the mice fed the HFD (213.08 ± 10.35 mg/dl) than those fed the lean diet (121.91 ± 2.26 mg/dl) as shown in Fig. 1B. Intra-peritoneal glucose tolerance tests shown in Fig. 2A indicate that the peaks of the blood glucose curves were significantly delayed (12 vs. 22 min) and much higher (414.6 ± 34.5 vs. 215 ± 13.3 mg/dl) in the mice fed the HFD than those fed the lean diet. Fig. 2B shows area under the curve.

Fig. 3 shows a schematic diagram of a simplified glucose-insulin system. The solid and dotted lines represent flow of glucose and insulin, respectively. Glucose (1 g/kg body weight) injected into the peritoneal cavity enters the plasma at a constant rate (k_0), then it flows from the plasma to the liver (k_4) and other tissues through both insulin-dependent (k_2) and −independent (k_3) pathways. In response to elevated levels of glucose in the plasma, pancreatic β-cells release insulin to the plasma (k_1). Insulin has a short plasma half-life (4–6 min) [18] and is removed by the liver, kidney, and muscles (k_6). Table 1 shows the summary of 9 parameters with appropriate units.

Arena^{TM} combined with the OptQuest^{TM} toolset was used to evaluate the mathematical model and optimally estimate the 8 rate constants in Eqs. (1)–(3) and plasma insulin levels. Arena^{TM} is based on the SIMAN programming language and

http://dx.doi.org/10.1016/j.heliyon.2017.e00310

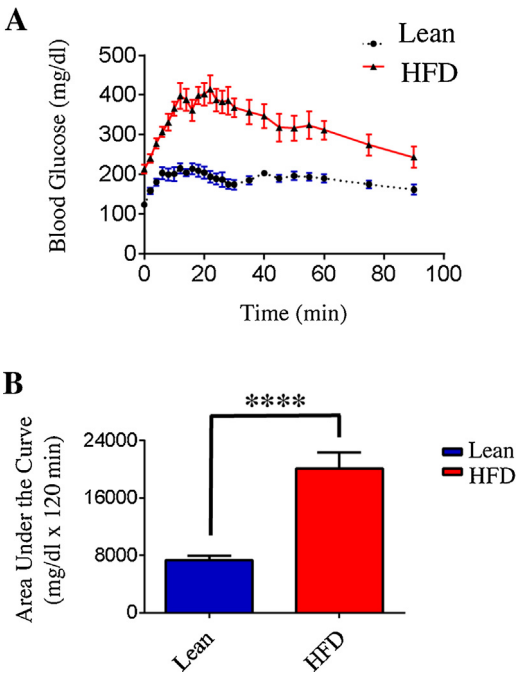

Fig. 2. (A) Plasma glucose levels during the intra-peritoneal glucose tolerance test (1 g/kg) for lean- and HFD-fed mice. Mice were fasted for 5 h and administered 1 g/kg glucose by intra-peritoneal injection using sterile 27 G disposable needles. Blood glucose levels were determined using Contour glucose meter collecting blood from the tip of the tail at 0 (prior to glucose injection) and every minute for the first 16 min, every 2 min for the next 14 min, every 5 min until 1 h, and then every 15 min until 2 h. (B) Total area under the curve for lean- and HFD-fed mice. Values are presented as means ± SEM. (n = 12).

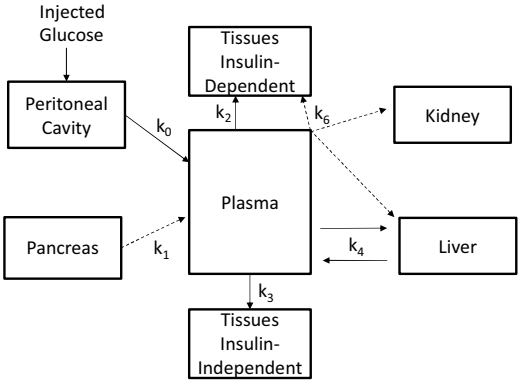

Fig. 3. The glucose-insulin system. The solid and dotted lines represent flow of glucose and insulin, respectively. Glucose (1 g/kg body weight) injected into the peritoneal cavity enters the plasma at a constant rate (k_0), then it flows from the plasma to the liver (k_4) and other tissues through both insulin-dependent (k_2) and −independent (k_3) pathways. In response to elevated levels of glucose in the plasma, pancreatic β-cells release insulin to the plasma (k_1). Insulin is removed by the liver, kidney, and muscles (k_6).

http://dx.doi.org/10.1016/j.heliyon.2017.e00310

Table 1. Model variables and parameters.

Term	Units	Type	Represents
G	(mg dl^{-1})	Variable	Plasma glucose concentration
I	(pmol l^{-1})	Variable	Plasma insulin concentration
D	(mg)	Variable	Amount of glucose in peritoneal cavity
K_0	(dl^{-1} min^{-1})	Constant	Rate constant of glucose entering blood from peritoneal cavity
K_1	(pmol dl min^{-1} mg^{-1} l^{-1})	Constant	Rate constant of pancreatic insulin secretion
K_2	(mg l dl^{-1} min^{-1} pmol $^{-1}$)	Constant	Rate constant of insulin-dependent glucose transfer to tissue
K_3	(mg dl^{-1} min^{-1})	Constant	Rate constant of insulin-independent glucose transfer to tissue
K_4	(mg l dl^{-1} min^{-1} pmol $^{-1}$)	Constant	Rate constant of liver glucose transfer
K_6	(min^{-1})	Constant	Rate constant of insulin clearance from blood
K_a	(min^{-1})	Constant	Rate constant of glucose leaving peritoneal cavity
I_{pi}	(pmol l^{-1})	Constant	Insulin concentration where liver switches from glucose release to absorption

is capable of handling both the discrete and continuous-time elements involved in this study [19]. It provides a block-based graphical interface with user-friendly flow-charts and permits access to background code if specific or unusual modifications are needed. The algorithm used in the simulation was designed by the authors to include continuous evaluation of glucose or insulin levels and rates, discrete disturbances and data point comparisons, optimization of parameter profiles, and graphical analysis and statistic collection. Fig. 4 shows an image of the graphical work environment and the Arena flowchart. Simulation tracks plasma glucose concentration, plasma insulin concentration, and peritoneal glucose concentration over time and bolus glucose injection rate. The 8 rate constants and plasma insulin levels were determined using a Visual Basic script, which sets the rate constant values according to the three differential equations and the initial values. Optimally fitting a 9 parameter set is a difficult task; however, the inclusion of OptQuest^{TM} in the Arena software package allowed us to estimate individual parameter with minimized sum of squared errors. The combination of parameters that resulted in the most accurate prediction for each mouse was generated after repeats of continuous tens of thousands of cycles of optimization and simulation.

Fig. 5 demonstrates the comparison between experimental and simulated glucose curves for the lean- and the HFD-fed mice. Fig. 5A and C show the experimental IPGTT data for the lean- and the HFD-fed mice, respectively. Fasting blood glucose level and the peak of the blood glucose curve were significantly lower in the lean diet-fed mouse compared to those in the HFD-fed mouse. The simulated data (Fig. 5B and D) fit accurately to the observed data for both lean and obese mice, validating the use of the mathematical model in mice at different metabolic states.

http://dx.doi.org/10.1016/j.heliyon.2017.e00310

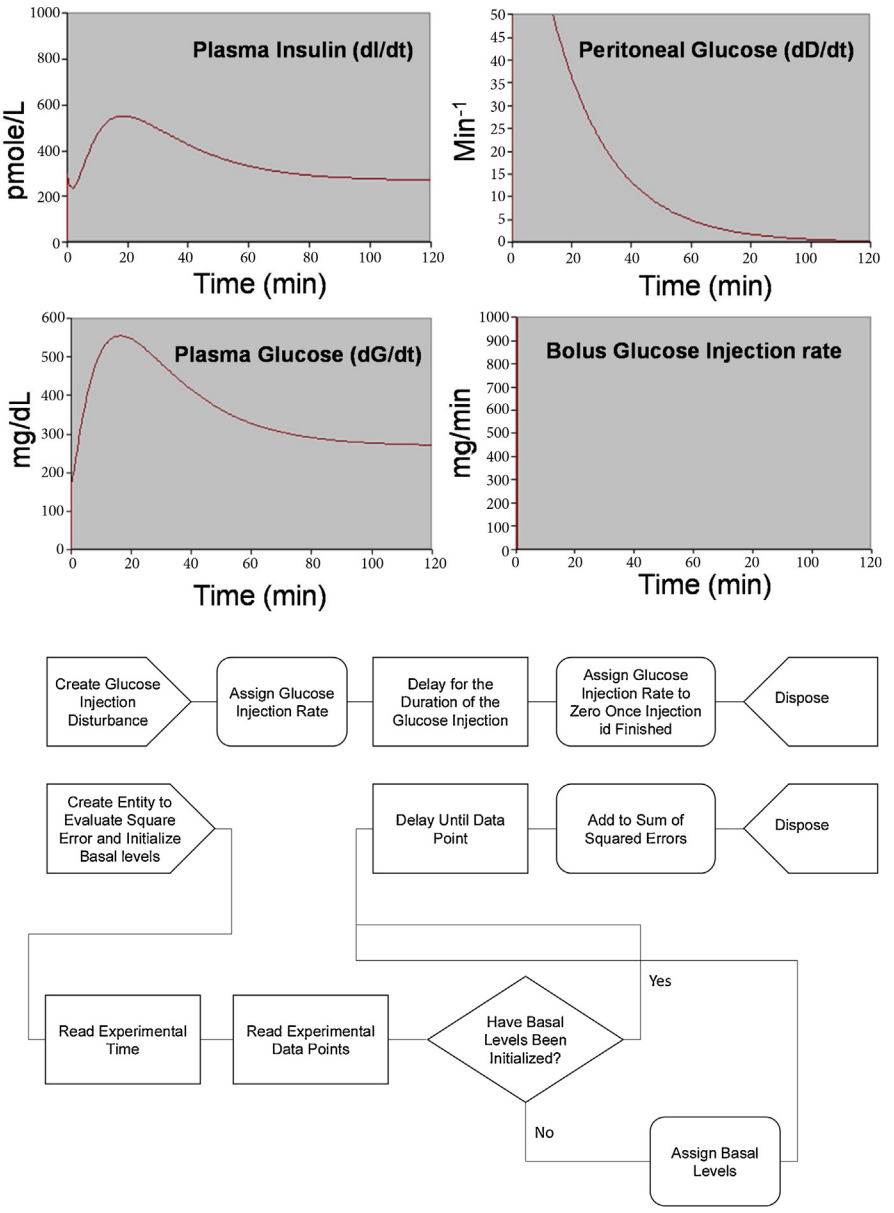

Fig. 4. The graphical work environment and the Arena flowchart. Simulation tracks plasma glucose concentration, plasma insulin concentration, and peritoneal glucose concentration over time, with glucose injection rate initially entered to the system. The 8 rate constants were determined using a Visual Basic script, which sets the rate constant values according to the three differential equations and the initial values. The OptQuest software was used to estimate individual parameter with minimized sum of squared errors. The combination of parameters that resulted in the most accurate prediction for each mouse was generated after repeats of continuous tens of thousands of cycles of optimization and simulation.

Fig. 6 shows that 5 out of 9 parameters were significantly different between the lean- and the HFD-fed mice. Fig. 6A shows that the plasma insulin levels were significantly higher in the HFD-fed mice (790.9 ± 83.6 pmol/l) than those in the lean diet-fed mice (218.1 ± 51.6 pmol/l), suggesting that the HFD-fed mice

http://dx.doi.org/10.1016/j.heliyon.2017.e00310

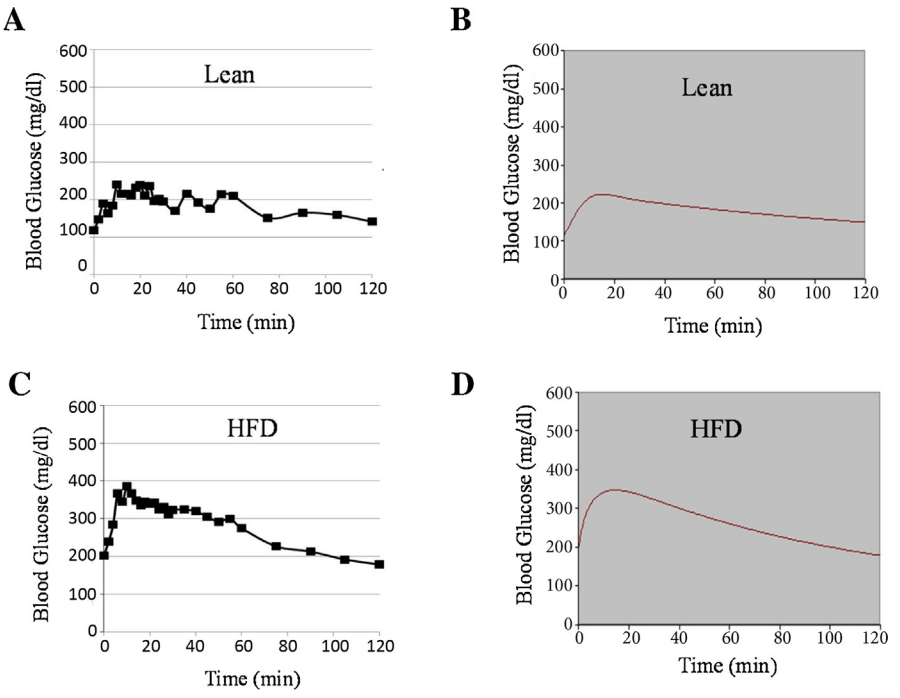

Fig. 5. Comparison between experimental and simulated glucose curves for the lean- and the HFD-fed mice. (A) and (C) show the experimental IPGTT data for the lean- and the HFD-fed mice, respectively. The simulated data (B) and (D) fit accurately to the observed data for both lean and obese mice, validating the use of the mathematical model in mice at different metabolic states.

developed hyperinsulinemia associated with the weight gain. It is well documented that pancreatic β-cell mass in rodents increases substantially to compensate insulin resistance associated with obesity, resulting in hyperinsulinemia [20, 21, 22]. The values for I_{pi}, insulin concentration where liver switches from glucose release to uptake, were significantly higher in the HFD-fed mice (850.4 ± 105.1 pmol/l) than those in the lean diet-fed mice (490.5 ± 62.3 pmol/l), suggesting that insulin resistance in the liver has ensued in the HFD-fed mice (Fig. 6B). Significantly lower values for k_4, the rate constant of liver glucose transfer, in the HFD-fed mice compared the lean diet-fed mice support insulin resistance in the liver of these mice (Fig. 6G). Furthermore, the values for k_2, the rate constant for insulin-dependent glucose transfer to tissues (muscles, adipocyte, etc.), were significantly lower in the HFD-fed mice compared to those in the lean diet-fed mice (Fig. 6E), providing additional evidence for insulin resistance in the HFD-fed mice. Finally, higher values for k_3, the rate constant for insulin-independent glucose transfer to tissues, in the HFD-fed mice than those in the lean diet-fed mice reflect increased body mass of the HFD-fed mice and perhaps increased number of glucose transporters that transport glucose into tissues in an insulin-independent manner (i.e. glucose transporter 1) due to expanded fat pads, blood volume (increased blood cells), etc. (Fig. 6F). Table 2 shows the summary of 9 parameters for the lean- and the HFD-

http://dx.doi.org/10.1016/j.heliyon.2017.e00310

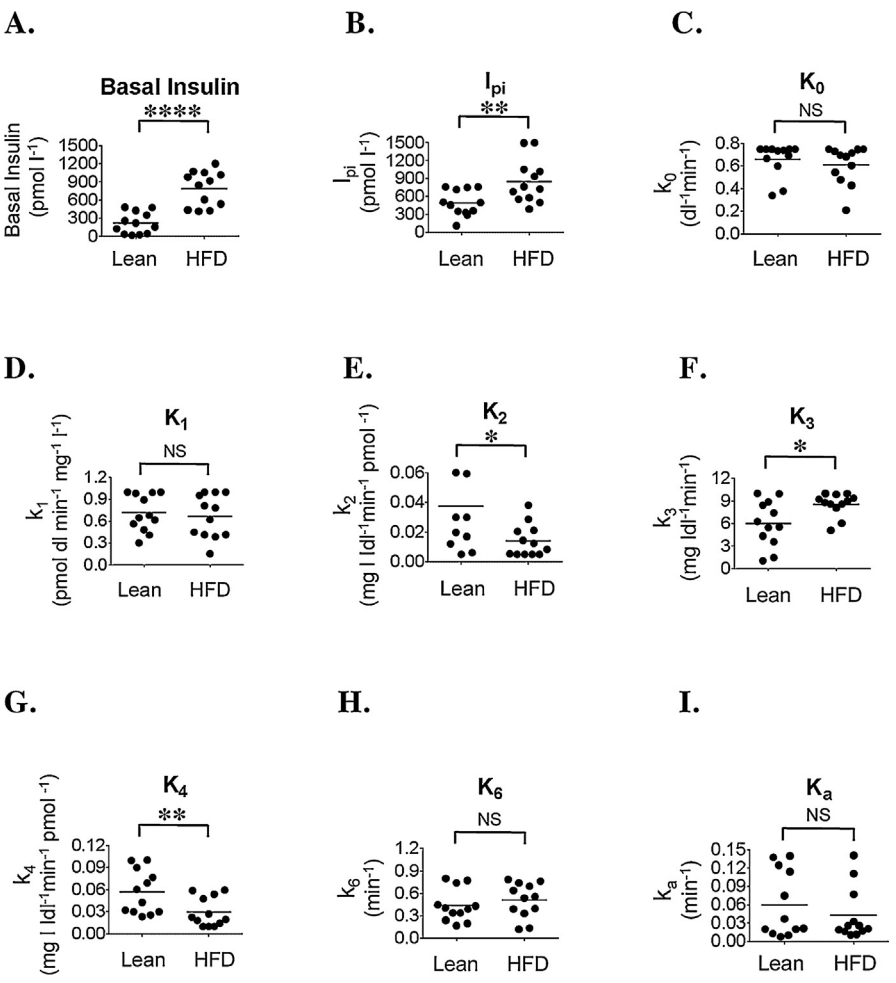

Fig. 6. Basal insulin levels, I_{pi}, and rate constants for lean- and HFD-fed mice. Values are presented as means ± SEM. (n = 12) NS denotes not significant.

fed mice. No statistical differences for k_1 (rate constant for pancreatic insulin secretion) and k_6 (rate constant for insulin clearance from blood) for lean- and HFD-fed mice may be due to increased β-cell mass, blood volume, and body mass in HFD-fed mice compared to lean diet-fed mice.

To determine the extent by which the variables are related to each other, correlogram plots (Table 3) and matrix plots (Fig. 7) of the 9 parameters for lean- and HFD-fed mice were obtained. Pearson's correlation coefficients (r) in bold and denoted by * in Table 3 show moderate to strong association between variables with P values <0.05. Interestingly, the data set for the lean mice showed no correlation among the various parameters except for a pair, k_2 and I_{pi} ($r = 0.586$, P value = 0.045), suggesting that insulin-dependent glucose uptake into the tissues such as muscles, adipocytes, and liver is correlated with insulin concentration where liver switches from glucose release to uptake. In contrast, the data set for the

http://dx.doi.org/10.1016/j.heliyon.2017.e00310

Table 2. Summary of 9 parameters for lean- and HFD-fed mice.

	Lean	HFD	P value
Basal Insulin (pmol l^{-1})	218.13 ± 51.58	790.95 ± 83.65	0.0001
I_{PI} (pmol l^{-1})	490.53 ± 62.34	850.37 ± 105.13	0.0083
K_0 (dl^{-1} min^{-1}; glucose entering blood from peritoneal cavity)	0.658 ± 0.042	0.611 ± 0.049	0.4423
K_1 (pmol dl min^{-1} mg^{-1} l^{-1}; pancreatic insulin secretion)	0.714 ± 0.073	0.665 ± 0.086	0.7449
K_2 (mg l dl^{-1} min^{-1} pmol $^{-1}$)	0.04 ± 0.007	0.01 ± 0.003	0.0165
K_3 (mg dl^{-1} min^{-1})	6.039 ± 0.881	8.561 ± 0.443	0.0447
K_4 (mg l dl^{-1} min^{-1} pmol $^{-1}$)	0.057 ± 0.008	0.029 ± 0.006	0.0067
K_6 (min^{-1})	0.440 ± 0.063	0.508 ± 0.067	0.6197
K_a (min^{-1})	0.060 ± 0.016	0.042 ± 0.012	0.6598

HFD-fed mice showed correlations among 4 different pairs; k_0 and k_1, (r = 0.686, P value = 0.014), k_1 and k_4 (r = 0.667, P value = 0.018), k_3 and k_2 (r = -0.681, P value = 0.015), and basal insulin and k_4 (r = 0.629, P value = 0.028). With weight gain, clustering of the rate constants were observed, especially between insulin levels and liver handling of glucose shown by correlations between k_1 and k_4, and basal insulin and k_4. As expected, a negative correlation between insulin-dependent (k_2) and Insulin-independent glucose uptake (k_3) was observed. A decrease in insulin sensitivity and an expansion of tissue mass are postulated to be responsible for the alterations in the k_2 and k_3 rate constants, respectively, and the negative correlations between the two. Of note, the rate constants, k_0 and k_1, were not significantly different between the lean- and the HFD-fed mice with the similar means and distributions of the data. However, a strong positive correlation between the rate constants was observed in the HFD-fed mice. As the demand for insulin increases due to an increase in insulin resistance in the HFD-fed mice, a stronger association between glucose amount in the blood and insulin secretion was perhaps necessary to compensate inefficient insulin action.

It is an interesting and noteworthy observation that obesity alters 5 out of 9 key metabolic parameters (Fig. 6) and promotes linear correlations between variables (Table 3). Correlations among the parameters, however, pose a challenge of obtaining unique parameter estimation. It is not unusual that a biological model contains a large number of parameters among which correlations exist [23]. In the lean healthy mice, interestingly, the parameters that determine the glucose-insulin homeostasis were mostly random and independent from each other (Table 3). In the HFD-fed mice, however, some of the parameters showed a trend of correlations. To determine whether the correlated parameters were non-identifiable, we conducted an additional sensitivity analysis by altering the initial parameters by 10%. The parameters converged to the identical values, suggesting

http://dx.doi.org/10.1016/j.heliyon.2017.e00310

http://dx.doi.org/10.1016/j.heliyon.2017.e00310

Table 3. Correlogram plots of the 9 parameters for lean- and HFD-fed mice.

Lean

	Ko	K1	K6	Ka	Basal Insulin	IPi	K2	K3	K4
Ko		-0.1089495	-0.1247493	0.3512817	0.0325186	-0.2304291	-0.4460203	0.01254778	0.003657366
K1	-0.1089495		0.3085915	0.1051752	-0.1098282	-0.1587495	-0.2971134	-0.3226861	-0.1388445
K6	-0.1247493	0.3085915		-0.01144793	-0.2103806	-0.306107	-0.2536101	0.2429865	-0.2014295
Ka	0.3512817	0.1051752	-0.01144793		-0.1294705	0.4805001	-0.002787193	-0.5413043	0.5143078
Basal Insulin	0.0325186	-0.1098282	-0.2103806	-0.1294705		0.1704797	0.5308409	0.04544165	0.3870685
IPi	-0.2304291	-0.1587495	-0.306107	0.4805001	0.1704797		**0.585531***	-0.4209763	0.5277556
K2	-0.4460203	-0.2971134	-0.2536101	-0.002787193	0.5308409	**0.585531***		-0.1123405	0.4346167
K3	0.01254778	-0.3226861	0.2429865	-0.5413043	0.04544165	-0.4209763	-0.1123405		-0.002460394
K4	0.003657366	-0.1388455	-0.2014295	0.5143078	0.3870685	0.5277556	0.4346167	-0.002460394	

HFD

	Ko	K1	K6	Ka	Basal Insulin	IPi	K2	K3	K4
Ko		**0.685577***	-0.2412862	0.1525934	0.521655	-0.4404172	-0.4343804	0.3498785	0.5625411
K1	**0.685577***		-0.4577924	-0.1323902	0.5056201	-0.5151732	-0.2073803	0.1018449	**0.666698***
K6	-0.2412862	-0.4577924		0.100917	0.09671769	0.08058558	0.2055724	0.1513771	-0.2927035
Ka	0.1525934	-0.1323902	0.100917		-0.04012257	0.1361282	-0.1191915	-0.1467494	-0.0571961
Basal Insulin	0.521655	0.5056201	0.09671769	-0.04012257		-0.09904491	-0.1182147	0.351851	**0.628890***
IPi	-0.4404172	-0.5151732	0.08058558	0.1361282	-0.09904491		0.254378	-0.3487022	-0.2316882
K2	-0.4343804	-0.2073803	0.2055724	-0.1191915	-0.1182147	0.254378		**-0.681394***	0.05840398
K3	0.3498785	0.1018449	0.1513771	-0.1467494	0.351851	-0.3487022	**-0.681394***		-0.2749244
K4	0.5625411	**0.666698***	-0.2927035	-0.0571961	**0.628890***	-0.2316882	0.05840398	-0.2749244	

A. Lean

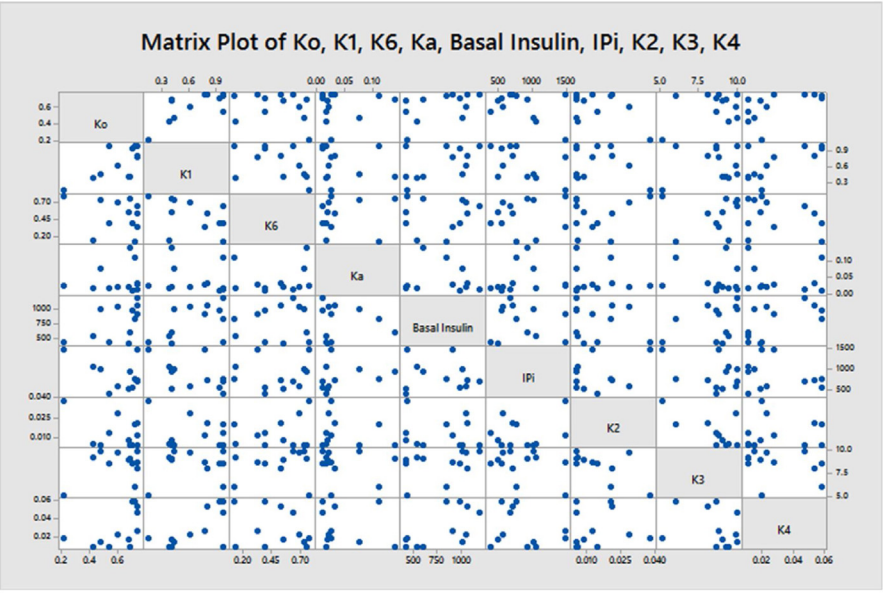

B. HFD

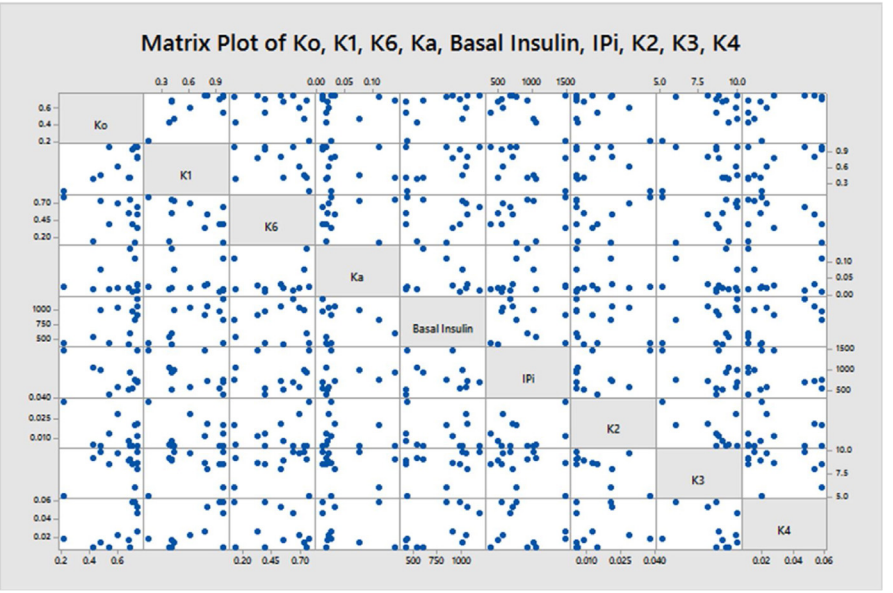

Fig. 7. Matrix plots of the 9 parameters for lean- (A) and HFD-fed mice (B). To determine the strength of the association between the variables, matrix plots of the parameters for lean- and HFD-fed mice were obtained.

that they were identifiable. Further investigations are needed to explore the issues of parameter correlations and their implications.

Over the years, a variety of mathematical models have contributed to better understanding of glucose-stimulated insulin release and the regulation of glucose-insulin homeostasis in the body. Mathematical modeling in addition to biochemical

http://dx.doi.org/10.1016/j.heliyon.2017.e00310

assays provided insights into 1) the first and the second phase of insulin release from the pancreatic β-cells by defining several pools of insulin secretory vesicles including the reserve pool, the docked vesicles, the immediately releasable vesicles, and the vesicles fused with cell membrane [24], and 2) pulsatile insulin secretion (oscillation), addressing questions how intra- and inter-islet β-cells synchronize insulin secretion [25, 26], and how each secretory unit reacts to circulating glucose, undergoes refractory period after secretion, and recruits other secretory units to increase the amount of the insulin secreted in response to elevated plasma glucose levels. Mathematical modeling of short-term (2–3 h) glucose-insulin dynamics after an external perturbation such as intravenous glucose injection (intravenous glucose tolerance test) [27, 28], oral glucose ingestion (oral glucose tolerance test) [29, 30, 31], or continuous infusions of glucose and insulin (euglycemic hyperinsulinemic clamp) [32, 33] has been used to aid diagnosis of glucose intolerance and T2DM. The minimal model proposed by Bergman et al. [34] in 1979 has been widely used as a clinical tool to assess insulin sensitivity of an individual and risk for T2DM. The minimal model, however, has drawbacks in not being able to estimate various parameters that determine glucose-insulin homeostasis. The model by Lomarte et al. that we have used in our study allows to estimate 8 different parameters (rate constants) and the plasma insulin levels that determine glucose-insulin homeostasis in different biological situations. Estimation of the plasma insulin levels especially in mice, of note, is very helpful because standard biochemical assays such as radioimmunoassay (RIA) for determination of plasma insulin levels requires substantial amount of blood (~70 μl) and a period of 2 days. The model by Lombarte et al. has been experimentally validated in healthy rats [14]. Furthermore, the model has been also used in *in vivo* measurement of fluoride effects on glucose homeostasis in rats [35]. The model is simple with relatively small number of unknown rate constants, yet represents the normal physiology of glucose-insulin homeostasis rather well at least in rodents. The less number of unknown rate constants in a model, the more advantageous because estimation of the rate constants is less depending on previous studies or other literature.

It is of great interest to assess alterations of the parameters that determine glucose-insulin homeostasis between lean and obese subjects. Our present study uniquely contributes to gaining insights into the differences in model parameters between lean and obese mice. Elevated plasma insulin levels (hyperinsulinemia), a decrease in insulin-dependent glucose uptake (k_2), and an increase in insulin-independent glucose uptake (k_3) in obese mice align well with previous studies [36, 37, 38]. In addition, liver handling of glucose in obese mice (elevated I_{pi} and decreased k_4) is a new finding which is not readily quantifiable. Alonso et al. determined first phase insulin secretion and the disposition index in lean and obese mice using frequently sampled intravenous glucose tolerance test (FSIVGTT) with mathematical

http://dx.doi.org/10.1016/j.heliyon.2017.e00310

modeling [39]. The authors, intriguingly, found that insulin secretion was the primary determinant for glucose disposal in lean mice, while glucose effectiveness and the disposition index more strongly predicted glucose disposal in obese mice, suggesting that the parameters responsible for glucose disposal kinetics varied between lean and obese mice [39]. Precise parameter estimations in lean and obese subjects may be helpful in designing strategies of therapeutic intervention, specifically targeting to prevent alterations in the parameters.

The methodology that we have established in this paper may be used as a valuable tool to study how the progression of obesity alters various parameters that determine glucose-insulin homeostasis. The precise change or time that converts from impaired glucose tolerance to frank diabetic condition may be pinpointed in an animal model. We also predict that each individual has a unique set of 9 parameters due to genetic diversity, metabolic differences, diet, etc. Thus, this information may be helpful in developing customized individual algorithms for closed-loop APD systems in the future. Furthermore, accurate assessment of rate constant for insulin secretion (assessment for β-cell function), insulin-dependent glucose-uptake (assessment for insulin resistance), or liver handling of glucose may also allow customized drug therapy targeting specific defect(s) of a patient, thus, delay the progression of the disease and its associated complications. In summary, the significance of this study is 1) validation of the mathematical modeling as a tool to study glucose-insulin homeostasis in individuals with different metabolic states, 2) provision of a new methodology to study the progression of obesity-induced metabolic alterations associated with T2DM in rodents, and 3) contribution to assessment of unique parameters of an individual, which may be used to develop customized algorithms for the APD systems.

Declarations

Author contribution statement

Michael Brenner: Conceived and designed the experiments; Performed the experiments; Analyzed and interpreted the data.

Sakineh Esmaeili Mohsen Abadi: Performed the experiments; Analyzed and interpreted the data.

Ramin Balouchzadeh, Michael Johns, Nehal Malik, Joshua Lee: Performed the experiments.

H. Felix Lee: Conceived and designed the experiments; Analyzed and interpreted the data.

Hoo Sang Ko: Analyzed and interpreted the data.

http://dx.doi.org/10.1016/j.heliyon.2017.e00310

Guim Kwon: Conceived and designed the experiments; Performed the experiments; Analyzed and interpreted the data; Wrote the paper.

Funding statement

This work was supported by NIH Grant 1R15DK094142-01A1 (GK) and SIUE internal grants (GK, HSK).

Competing interest statement

The authors declare no conflict of interest.

Additional information

No additional information is available for this paper.

References

[1] A. Bruni, B. Gala-Lopez, A.R. Pepper, N.S. Abualhassan, A.J. Shapiro, Islet cell transplantation for the treatment of type 1 diabetes: recent advances and future challenges, Diabetes Metab. Syndr. Obes. 7 (2014) 211–223.

[2] F.J. Cameron, D.K. Wherrett, Care of diabetes in children and adolescents: controversies, changes, and consensus, Lancet 385 (2015) 2096–2106.

[3] G. Boden, Effects of free fatty acids (FFA) on glucose metabolism: significance for insulin resistance and type 2 diabetes, Exp. Clin. Endocrinol Diabetes 111 (2003) 121–124.

[4] G. Pilon, A. Charbonneau, P.J. White, P. Dallaire, M. Perreault, S. Kapur, A. Marette, Endotoxin mediated-iNOS induction causes insulin resistance via ONOO(−) induced tyrosine nitration of IRS-1 in skeletal muscle, PLoS One 5 (2010) e15912.

[5] E. Bachar, Y. Ariav, M. Ketzinel-Gilad, E. Cerasi, N. Kaiser, G. Leibowitz, Glucose amplifies fatty acid-induced endoplasmic reticulum stress in pancreatic beta-cells via activation of mTORC1, PLoS One 4 (2009) e4954.

[6] U. Ozcan, Q. Cao, E. Yilmaz, A.H. Lee, N.N. Iwakoshi, E. Ozdelen, G. Tuncman, C. Gorgun, L.H. Glimcher, G.S. Hotamisligil, Endoplasmic reticulum stress links obesity, insulin action, and type 2 diabetes, Science 306 (2004) 457–461.

[7] A.E. Butler, J. Janson, S. Bonner-Weir, R. Ritzel, R.A. Rizza, P.C. Butler, Beta-cell deficit and increased beta-cell apoptosis in humans with type 2 diabetes, Diabetes 52 (2003) 102–110.

 http://dx.doi.org/10.1016/j.heliyon.2017.e00310

[8] J. Rahier, Y. Guiot, R.M. Goebbels, C. Sempoux, J.C. Henquin, Pancreatic beta-cell mass in European subjects with type 2 diabetes, Diabetes Obes. Metab. 10 (Suppl 4) (2008) 32–42.

[9] United Kingdom Prospective Diabetes Study, 24: a 6-year, randomized, controlled trial comparing sulfonylurea, insulin, and metformin therapy in patients with newly diagnosed type 2 diabetes that could not be controlled with diet therapy. United Kingdom Prospective Diabetes Study Group, Ann. Intern. Med. 128 (1998) 165–175.

[10] U.K. prospective diabetes study, 16. Overview of 6 years' therapy of type II diabetes a progressive disease U.K. Prospective Diabetes Study Group, Diabetes 44 (1995) 1249–1258.

[11] S.E. Kahn, S.M. Haffner, M.A. Heise, W.H. Herman, R.R. Holman, N.P. Jones, B.G. Kravitz, J.M. Lachin, M.C. O'Neill, B. Zinman, G. Viberti, Glycemic durability of rosiglitazone, metformin, or glyburide monotherapy, N. Engl. J. Med. 355 (2006) 2427–2443.

[12] D.R. Matthews, J.P. Hosker, A.S. Rudenski, B.A. Naylor, D.F. Treacher, R.C. Turner, Homeostasis model assessment: insulin resistance and beta-cell function from fasting plasma glucose and insulin concentrations in man, Diabetologia 28 (1985) 412–419.

[13] E.Y. Lee, S. Hwang, S.H. Lee, Y.H. Lee, A.R. Choi, Y. Lee, B.W. Lee, E.S. Kang, C.W. Ahn, B.S. Cha, H.C. Lee, Postprandial C-peptide to glucose ratio as a predictor of beta-cell function and its usefulness for staged management of type 2 diabetes, J. Diabetes Investig. 5 (2014) 517–524.

[14] M. Lombarte, M. Lupo, G. Campetelli, M. Basualdo, A. Rigalli, Mathematical model of glucose-insulin homeostasis in healthy rats, Math. Biosci. 245 (2013) 269–277.

[15] H. Karasawa, S. Nagata-Goto, K. Takaishi, Y. Kumagae, A novel model of type 2 diabetes mellitus based on obesity induced by high-fat diet in BDF1 mice, Metabolism 58 (2009) 296–303.

[16] F. Maher, T.M. Davies-Hill, P.G. Lysko, R.C. Henneberry, I.A. Simpson, Expression of two glucose transporters, GLUT1 and GLUT3, in cultured cerebellar neurons: Evidence for neuron-specific expression of GLUT3, Mol. Cell. Neurosci. 2 (1991) 351–360.

[17] I.A. Simpson, D. Dwyer, D. Malide, K.H. Moley, A. Travis, S.J. Vannucci, The facilitative glucose transporter GLUT3: 20 years of distinction, Am. J. Physiol. Endocrinol. Metab. 295 (2008) E242–253.

http://dx.doi.org/10.1016/j.heliyon.2017.e00310

[18] W.C. Duckworth, R.G. Bennett, F.G. Hamel, Insulin degradation: progress and potential, Endocr. Rev. 19 (1998) 608–624.

[19] W.D. Kelton, R.P. Sadowski, N.B. Sweets, Simulation with Arena, fifth ed., McGraw-Hill, 2010.

[20] J.C. Bruning, J. Winnay, S. Bonner-Weir, S.I. Taylor, D. Accili, C.R. Kahn, Development of a novel polygenic model of NIDDM in mice heterozygous for IR and IRS-1 null alleles, Cell 88 (1997) 561–572.

[21] R.L. Hull, K. Kodama, K.M. Utzschneider, D.B. Carr, R.L. Prigeon, S.E. Kahn, Dietary-fat-induced obesity in mice results in beta cell hyperplasia but not increased insulin release: evidence for specificity of impaired beta cell adaptation, Diabetologia 48 (2005) 1350–1358.

[22] A.V. Matveyenko, J.D. Veldhuis, P.C. Butler, Adaptations in pulsatile insulin secretion, hepatic insulin clearance, and beta-cell mass to age-related insulin resistance in rats, Am. J. Physiol. Endocrinol. Metab. 295 (2008) E832–841.

[23] P. Li, Q.D. Vu, Identification of parameter correlations for parameter estimation in dynamic biological models, BMC Syst. Biol. 7 (2013) 91.

[24] A. Bertuzzi, S. Salinari, G. Mingrone, Insulin granule trafficking in beta-cells: mathematical model of glucose-induced insulin secretion, Am. J. Physiol. Endocrinol. Metab. 293 (2007) E396–409.

[25] M.G. Pedersen, R. Bertram, A. Sherman, Intra- and inter-islet synchronization of metabolically driven insulin secretion, Biophys. J. 89 (2005) 107–119.

[26] M.G. Pedersen, A. Corradin, G.M. Toffolo, C. Cobelli, A subcellular model of glucose-stimulated pancreatic insulin secretion, Philos. Trans. A Math. Phys. Eng. Sci. 366 (2008) 3525–3543.

[27] A. Basu, C. Dalla Man, R. Basu, G. Toffolo, C. Cobelli, R.A. Rizza, Effects of type 2 diabetes on insulin secretion, insulin action, glucose effectiveness, and postprandial glucose metabolism, Diabetes care 32 (2009) 866–872.

[28] A. Caumo, C. Cobelli, Hepatic glucose production during the labeled IVGTT: estimation by deconvolution with a new minimal model, Am. J. Physiol. 264 (1993) E829–841.

[29] E. Ackerman, L.C. Gatewood, J.W. Rosevear, G.D. Molnar, Model studies of blood-glucose regulation, Bull. Math. Biophys. 27 (Suppl 1) (1965) 21–37.

[30] L.C. Gatewood, E. Ackerman, J.W. Rosevear, G.D. Molnar, T.W. Burns, Tests of a mathematical model of the blood-glucose regulatory system, Comput. Biomed. Res. 2 (1968) 1–14.

 http://dx.doi.org/10.1016/j.heliyon.2017.e00310

[31] A. Caumo, R.N. Bergman, C. Cobelli, Insulin sensitivity from meal tolerance tests in normal subjects: a minimal model index, J. Clin. Endocrinol. Metab. 85 (2000) 4396–4402.

[32] R.A. DeFronzo, J.D. Tobin, R. Andres, Glucose clamp technique: a method for quantifying insulin secretion and resistance, Am. J. Physiol. 237 (1979) E214–223.

[33] U. Picchini, A. De Gaetano, S. Panunzi, S. Ditlevsen, G. Mingrone, A mathematical model of the euglycemic hyperinsulinemic clamp, Theor. Biol. Med. Model. 2 (2005) 44.

[34] R.N. Bergman, Y.Z. Ider, C.R. Bowden, C. Cobelli, Quantitative estimation of insulin sensitivity, Am. J. Physiol. 236 (1979) E667–677.

[35] M. Lombarte, B.L. Fina, P.M. Lupion, M. Lupo, A. Rigalli, In vivo measurement of fluoride effects on glucose homeostasis: an explanation for the decrease in intelligence quotient and insulin resistance induced by fluoride, Fluoride 49 (2016) 204–210.

[36] M.S. Winzell, B. Ahren, The high-fat diet-fed mouse: a model for studying mechanisms and treatment of impaired glucose tolerance and type 2 diabetes, Diabetes 53 (Suppl 3) (2004) S215–219.

[37] R. Buettner, C.B. Newgard, C.J. Rhodes, R.M. O'Doherty, Correction of diet-induced hyperglycemia, hyperinsulinemia, and skeletal muscle insulin resistance by moderate hyperleptinemia, Am. J. Physiol. Endocrinol. Metab. 278 (2000) E563–569.

[38] R. Burcelin, V. Crivelli, A. Dacosta, A. Roy-Tirelli, B. Thorens, Heterogeneous metabolic adaptation of C57BL/6J mice to high-fat diet, Am. J. Physiol. Endocrinol. Metab. 282 (2002) E834–842.

[39] L.C. Alonso, Y. Watanabe, D. Stefanovski, E.J. Lee, S. Singamsetty, L.C. Romano, B. Zou, A. Garcia-Ocana, R.N. Bergman, C.P. O'Donnell, Simultaneous measurement of insulin sensitivity, insulin secretion, and the disposition index in conscious unhandled mice, Obesity 20 (2012) 1403–1412.

http://dx.doi.org/10.1016/j.heliyon.2017.e00310